ЖЭТФ, 2006, том 129, вып. 2, стр. 254–267

SINGLE-SPIN ASYMMETRIES IN THE BETHE – HEITLER PROCESS $e^- + p \to e^- + \gamma + p$ INDUCED BY LOOP CORRECTIONS

A. V. Afanasev [a], ***M. I. Konchatnij*** [b], ***N. P. Merenkov*** [b*]

[a] *Jefferson Lab, Newport News, VA 23606, USA*

[b] *National Scientific Center «Kharkov Institute of Physics and Technology» 61108, Kharkov, Ukraine*

Submitted 28 July 2005

The single-spin beam and target asymmetries in the hard electroproduction process $e^- + p \to e^- + \gamma + p$ induced by the loop radiative corrections to the vertex part of lepton interaction are considered. The physical reason for the appearance of such a kind of asymmetries is a nonzero imaginary part of the amplitude (on the level of radiative corrections) caused by diagrams with a photon radiation by the outgoing electron. We calculate the single-spin beam and target asymmetries at a longitudinally polarized electron beam or at arbitrary polarizations of the target proton for the CLAS and HERMES experimental conditions.

PACS: 12.20.-m, 13.40.-f, 13.60.-r, 13.60.Hb, 13.88.+e

1. INTRODUCTION

It has been well known during a long time that the parity-conserving single-spin beam and target correlations in elastic electron–proton scattering and the radiative ($ee'\gamma$) reaction can be used to extract information about the virtual Compton scattering (VCS) amplitude. This amplitude is a very important physical quantity, which has triggered a significant experimental and theoretical activity.

Below the pion production threshold, it allows accessing generalized polarizabilities of the proton, which are defined by quadratic terms in the expansion of the VCS amplitude in the photon momenta [1, 2]. Different theoretical approaches and models have been suggested to describe the proton polarizabilities [3–7] and the first low-energy dedicated VCS experiments were performed at MAMI [8] and Jlab [9].

In the region of large energies and photon virtualities, VCS is usually referred to as deeply virtual Compton scattering (DVCS). The corresponding DVCS amplitude can be parameterized by new generalized parton distributions [10–12], commonly termed the skewed parton distributions. The pioneering papers cited above have stimulated considerable theoretical efforts in this field (see, e.g., reviews [13] and the references therein) and experimental studies of related hard electroproduction [14, 15].

In elastic scattering, the VCS amplitude enters through the two-photon exchange diagram (TPE) with two off-shell photons. The cross section and parity-conserved spin–spin correlations in this case are sensitive only to the real part of this diagram and, therefore, to the real part of the double off-shell VCS amplitude. The VCS-dependent contributions to these observables have the status of the first-order electromagnetic radiative correction to the Born values and have been calculated suggesting elastic [16] and inelastic [17] intermediate hadronic states in the TPE diagram. On the other hand, the single-spin normal asymmetry probes only the imaginary part of the TPE amplitude for both beam and target normal (perpendicular to the reaction plane) polarizations [18] and is equal to zero if the TPE diagram is excluded. Recent theoretical calculations suitable for different kinematical regions have been performed in [19–21]. Although the respective effect is very small (of the order of a few ppm), it can be measured in different experimental laboratories [22]. We also note that if the electron beam or the target proton is polarized in the reaction plane, the parity-conserving single-spin asymmetry for elastic scattering is strictly zero.

*E-mail: merenkov@kipt.kharkov.ua

Nevertheless, a nonzero asymmetry of this kind can manifest itself in the process with three (and more) final particles provided that all the final-particle 3-momenta do not belong to the same plane. The simplest process of this type probing the VCS amplitude is the reaction $(ee'\gamma)$ mentioned above,

$$e^-(k_1) + p(p_1) \to e^-(k_2) + \gamma(k) + p(p_2), \qquad (1)$$

which is described in the Born approximation by diagrams in Fig. 1.

The diagrams in Fig. 1*a, b* correspond to the well-known Bethe–Heitler (BH) amplitude, in which the hadronic structure is described by ordinary electromagnetic form factors of the proton. The diagrams in Fig. 1*c, d* contain a VCS block with one virtual and one real photon. Below, we refer to them as the VCS amplitude. In general, the VCS amplitude includes both the real and imaginary parts, in contrast to the BH amplitude, which is purely real.

The parity-conserving single-spin asymmetries in process (1) with an arbitrarily polarized electron beam or target proton are proportional to the real part of the whole amplitude times its imaginary part that arises due to the VCS amplitude in Fig. 1*d*. As a rule, the BH amplitude dominates and the effect caused by the real part of the VCS one is a few times smaller. In spite of this circumstance, experimental data for single-spin correlations can be used to extract information about both real and imaginary parts of the VCS amplitude.

We note that the one-loop correction to the lepton part of the BH amplitude with radiation of a photon by the outgoing electron can generate an additional contribution to the single-spin asymmetries due to the interference of the diagrams in Fig. 1*a, b* and those in Fig. 2. The knowledge of the radiative correction is very important in analyzing experimental data because the first absolute measurement of the VCS cross section on a nucleon performed at MAMI [8] indicates a large QED radiative correction of the order 20 %. There is another class of diagrams at the level of radiative corrections that also leads to a nonzero imaginary part — the so-called box-type diagrams. Estimation of their contribution to the observables in process (1) and to the single-spin asymmetries, in particular, is a large theoretical problem because it requires a model for the VCS amplitude. In comprehensive work [23] devoted to the study of radiative corrections in this process, the authors used an approach recently developed in [16], excluding inelastic intermediate hadronic states in model-dependent box-type diagrams. By means of semianalytic (mainly numerical) calculations, they have obtained different observables accounting for the radiative corrections (also including single-spin beam asymmetry), where model-independent contribution caused by the diagrams in Fig. 2 mix with model-dependent ones.

In this paper, we obtain analytic expressions for model-independent contributions to the single-spin beam and target asymmetries in the BH process that appear due to one-loop vertex corrections to the BH amplitude in Fig. 1*b*. The knowledge of these contributions is necessary in order to be sure in determination of the model-dependent pieces from experimental data, which already arise at the Born level and are caused by the VCS amplitude. The corresponding result turns out to be simple enough to include it in Monte Carlo generators for the analysis of VCS experiments. In our calculations, we used analytic formulas for the one-loop-corrected Compton tensor in electrodynamics in the scattered channel obtained in [24] for the longitudinally polarized electrons and in [25] in the unpolarized case. We note that the results in Ref. [25] were recently confirmed in [26], where such a Compton tensor was calculated independently for the annihilation channel and it was shown that both tensors are related via analytic continuation.

2. KINEMATICAL VARIABLES AND THE PHASE-SPACE FACTOR

To describe the physical observables in process (1), the three dimensionless variables

$$x = -\frac{(k_1-k_2)^2}{2p_1(k_1-k_2)}, \quad y = \frac{2p_1(k_1-k_2)}{V}, \quad \rho = -\frac{(p_1-p_2)^2}{V}, \quad V = 2p_1k_1 \qquad (2)$$

and two azimuthal angles in the target proton rest frame are typically used. One of them, Φ, is simply the angle between the leptonic and hadronic planes as shown in Fig. 3 for two different choices of the z axis: opposite to the direction of $\mathbf{q}_1 = \mathbf{k}_1 - \mathbf{k}_2$ (Fig. 3*a*) [27] and along the direction of $\mathbf{k}_1$ (Fig. 3*b*) (in what follows, we refer to these systems as K and $\hat{K}$, respectively). The other one, Ψ, is the azimuthal angle of an arbitrary target polarization 3-vector provided that the xz plane is defined by the outgoing electron 3-momentum. The detailed consideration of transformations between the different target polarization states and between the angles Ψ and $\hat{\Psi}$ can be found in [28]. Here, we emphasize that we consider only those target polarizations that can be expressed through the particle 4-momenta (their physical content is given in Sec. 4 below). This

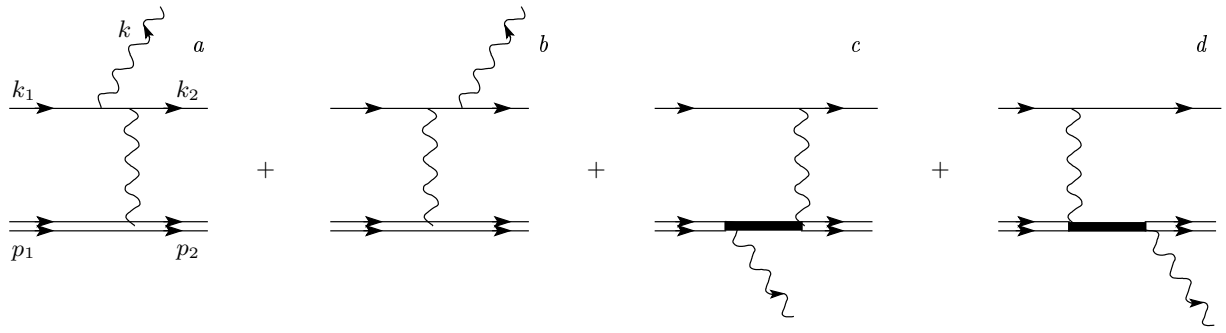

Fig. 1. Born diagrams for process (1). The solid part of the proton line indicates that together with elastic intermediate hadronic state, the inelastic ones must be taken into account. These last provide the imaginary part of diagram d

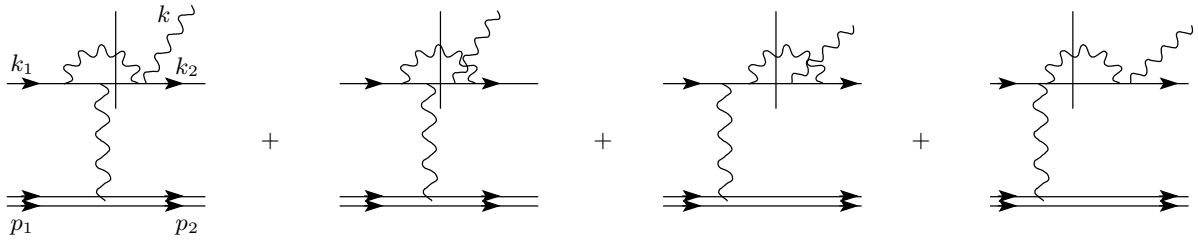

Fig. 2. One-loop corrections to diagram Fig. 1 b that generate a nonzero imaginary part of the BH amplitude in the order α

means that our target polarization asymmetries are independent of the angle Ψ and we can perform trivial integration over it.

The energies and the 3-momentum modules of the particles are independent of the choice of the z axis; with the electron mass neglected, they are given by

$$\begin{aligned} &\varepsilon_1 = \beta, \quad \varepsilon_2 = \beta(1-y), \quad q_{10} = \beta y, \\ &E_2 = \beta(2\tau+\rho), \quad |\mathbf{p}_2| = \beta\sqrt{\rho(4\tau+\rho)}, \end{aligned} \tag{3}$$

$$|\mathbf{q}_1| = \beta\sqrt{y^2+4xy\tau}, \quad \beta = \sqrt{\frac{V}{4\tau}}, \quad \tau = \frac{M^2}{V},$$

where ε_1 (ε_2) is the energy of the incoming (outgoing) electron and E_2 ($\mathbf{p}_2$) is the energy (3-momentum) of the recoil proton.

In contrast to the energies, the scattering angles depend on the choice of the z-axis direction. For the system K, we have

$$\begin{aligned} \cos\theta_e &= -\frac{y(1-y-2x\tau)}{(1-y)\sqrt{y^2+4xy\tau}}, \\ \cos\theta_p &= -\frac{y\rho+2\tau(\rho+xy)}{\sqrt{\rho(4\tau+\rho)(y^2+4xy\tau)}}, \end{aligned} \tag{4}$$

and for the system $\hat{K}$,

$$\begin{aligned} \cos\hat{\theta}_e &= \frac{1-y-2xy\tau}{1-y}, \quad \cos\hat{\theta}_p = \frac{\rho+2z\tau}{\sqrt{\rho(4\tau+\rho)}}, \\ z &= 1-\frac{2k_1p_2}{V}, \end{aligned} \tag{5}$$

where θ_e and θ_p are the electron and proton scattering angles in the system K; $\hat{\theta}_e$ and $\hat{\theta}_p$ are the same angles in the system $\hat{K}$, and we introduced, for convenience, a new dimensionless quantity z that has to be expressed through the azimuthal angle and invariant variables (2) in the final results.

The photon is usually not recorded experimentally, and therefore we have to eliminate the photon 4-momentum from the phase space of final particles by means of the overall $\delta^{(4)}$-function. Thus, we have to define

$$dF = \frac{d^3k_2}{\varepsilon_2}\,\frac{d^3p_2}{E_2}\delta(k^2). \tag{6}$$

Elimination of $\delta(k^2)$ is trivial in the system K,

$$\delta(k^2)\,d\cos\theta_p = \frac{1}{2|\mathbf{q}_1||\mathbf{p}_2|},$$

which leads to

$$dF_q = \frac{\pi V}{2}\,\frac{y}{\sqrt{y^2+4xy\tau}}dx\,dy\,d\rho\,d\Phi. \tag{7}$$

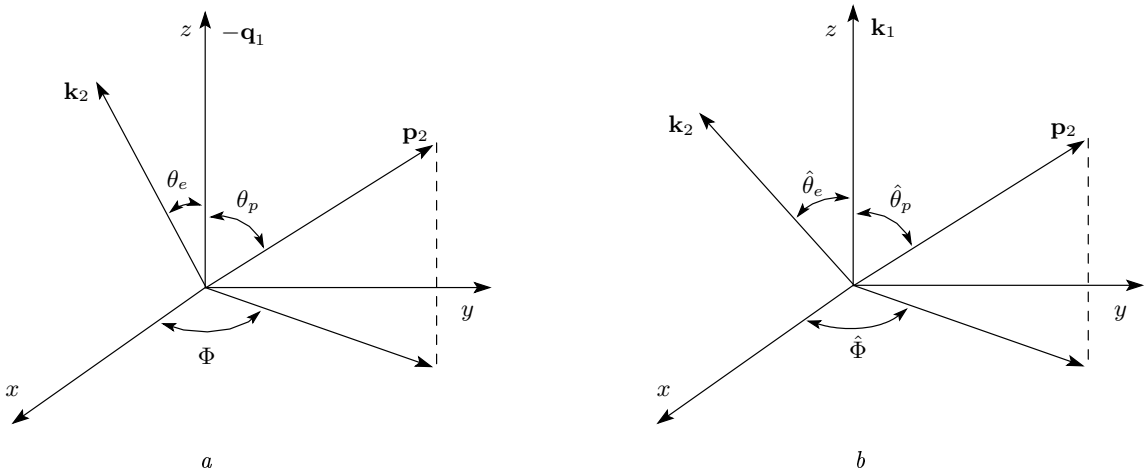

Fig. 3. Definition of angles in laboratory system with differently chosen coordinate axes

For the system $\hat{K}$, the equation $k^2 = 0$ represents a relation between the variables x, y, ρ, Φ, and $\cos\hat{\theta}_p$ that is nonlinear with respect to $\cos\hat{\theta}_p$, namely,

$$\frac{k^2}{V} = -\alpha - \beta\cos\hat{\Phi}\sqrt{1-\cos^2\hat{\theta}_p} + \gamma\cos\hat{\theta}_p = 0, \quad (8)$$

where α, β, and γ are always positive and

$$\alpha = xy+\rho+\frac{\rho y}{2\tau}, \quad \beta = \frac{1}{\tau}\sqrt{xy\rho\tau(4\tau+\rho)(1-y-xy\tau)},$$

$$\gamma = \frac{y(1+2x\tau)}{2\tau}\sqrt{\rho(4\tau+\rho)}.$$

We note that in terms of the invariant variable z, this equation is equivalent to

$$\cos\hat{\Phi} = -\frac{\rho(1-xy)+xy-yz(1+2x\tau)}{2\sqrt{xy(1-y-xy\tau)[\rho(1-z)-z^2\tau]}}.$$

To eliminate the δ-function in the phase space in (6), we now have to find all possible solutions of Eq. (8), taking into account that in accordance with Eq. (5), the quantity $\cos\hat{\theta}_p$ is positive.

Simple analysis leads to the following conclusion.

i) If $\cos\hat{\Phi} > 0$, there is only one solution provided that $\gamma > \alpha$ (at $\gamma < \alpha$, the solution is absent).

ii) If $\cos\hat{\Phi} < 0$ and $\gamma > \alpha$, the required solution exists if $\alpha > \beta|\cos\hat{\Phi}|$. With these conditions, we have

$$\cos\hat{\theta}_+ = \frac{1}{\gamma^2+\beta^2\cos^2\hat{\Phi}} \times$$
$$\times\left(\alpha\gamma+\beta\cos\hat{\Phi}\sqrt{\gamma^2-\alpha^2+\beta^2\cos^2\hat{\Phi}}\right), \quad \gamma > \alpha, \quad (9)$$

for an arbitrary sign of $\cos\hat{\Phi}$. It is clear that in this case, all values of the azimuthal angle are possible. We also note that the condition $\gamma > \alpha$ restricts the quantity ρ at fixed x and y in the range $\rho_1 < \rho < \rho_2$ such that $\rho_1 > \rho_-$ and $\rho_2 < \rho_+$ (for $\rho_\pm$, see Eq. (17) below).

iii) If $\gamma < \alpha$ and $\cos\hat{\Phi} < 0$, only those azimuth angles are allowed for which

$$|\cos\hat{\Phi}| > \frac{\sqrt{\alpha^2-\gamma^2}}{\beta}.$$

In the case where

$$\beta|\cos\hat{\Phi}| < \alpha < \sqrt{\gamma^2+\beta^2\cos^2\hat{\Phi}},$$

we have two different solutions $\cos\theta_\pm$ with both signs in front of the second term in the right-hand side of Eq. (9).

iv) Finally, if $\alpha < \beta|\cos\hat{\Phi}|$, the quantity $\cos\theta_+$ becomes negative and only $\cos\theta_-$ survives.

Therefore, in general, we must account for two different roots of Eq. (8), which leads to

$$\delta(k^2)\,d\cos\hat{\theta}_p = \frac{dz}{F_z}\left[\delta(z-z_+)+\delta(z-z_-)\right], \quad (10)$$

$$F_z = y(1+2x\tau)+(\rho+2z\tau)\cos\hat{\Phi}\sqrt{\frac{xy(1-y-xy\tau)}{\rho-z\rho-z^2\tau}},$$

and the quantities $z_\pm$ are simply expressed through $\cos\theta_\pm$ as

$$z_\pm = \frac{\cos\theta_\pm - a}{b}, \quad a = \frac{\rho}{\sqrt{\rho(4\tau+\rho)}}, \quad b = \frac{2\tau}{\sqrt{\rho(4\tau+\rho)}}.$$

In terms of the variables used, they become

$$z_\pm = \frac{A \pm B\cos\hat{\Phi}}{D}, \quad (11)$$

where the coefficients A, B, and D are even functions of $\cos\hat{\Phi}$,

$$A = y\Big[(1+2x\tau)(\rho+xy(1-\rho))-2x\rho(1-y-xy)\cos^2\hat{\Phi}\Big],$$

$$B = 2\sqrt{xy(1-y-xy\tau)H},$$

$$H = y\rho(1+2x\tau)\Big[y(1+2x\tau)-\rho-xy(1-\rho)\Big]-$$
$$-\tau[\rho+xy(1-\rho)]^2+xy\rho(1-y-xy\tau)(4\tau+\rho)\cos^2\hat{\Phi}, \quad (12)$$

$$D = y^2(1+2x\tau)^2+4xy\tau(1-y-xy\tau)\cos^2\hat{\Phi}.$$

We note that $z_+ \leftrightarrow z_-$ under the substitution $\hat{\Phi}\to\pi\pm\hat{\Phi}$. Thus, for the system $\hat{K}$, we have

$$dF_k = \frac{\pi V}{2}y\,dx\,dy\,d\rho\,d\hat{\Phi}\frac{dz}{F_z}\left[\delta(z-z_+)+\delta(z-z_-)\right]. \quad (13)$$

Here, we emphasize a principal distinction in the description of any polarization observable by means of the coordinate systems K and $\hat{K}$. In the first case, the same factors in polarization-dependent and unpolarized parts of the cross section can always be eliminated in their ratio. In the second case, this cannot be done under condition iii) because every z-dependent factor actually represents the sum of two terms weighted with different functions. To clarify this point, we imagine for a moment that the cross section has the form

$$d\sigma = \Big(U+P\Big)\,G\,dF, \quad (14)$$

where the function U (P) describes unpolarized (polarization-dependent) events and depends on invariant variables x, y, ρ, and z. Then for the system K, the polarization asymmetry is the ratio

$$A_q = \frac{P}{U}, \quad (15)$$

where we have to express the invariant variable z through x, y, ρ, and $\cos\Phi$ as (see also [27])

$$z = \frac{1}{y+4x\tau}\Big[2K\cos\Phi+2x\tau(xy+\rho)+$$
$$+xy+\rho(1+xy-2x)\Big], \quad (16)$$

$$K^2 = \frac{x(1-y-xy\tau)(y-xy+\tau)(\rho_+-\rho)(\rho-\rho_-)}{y}.$$

The quantities $\rho_\pm$ in the last expression have the meaning of the maximum and minimum values of ρ at fixed x and y,

$$\rho_\pm = \frac{y}{2[y(1-x)+\tau]}\times$$
$$\times\left[(1-x)\left(y\pm\sqrt{y^2+4xy\tau}\right)+2x\tau\right]. \quad (17)$$

For the system $\hat{K}$, simple substitution of Eq. (13) in cross section (14) defines the polarization asymmetry under condition iii) as

$$A_k = \frac{P(z_+)G(z_+)F_z(z_-)+P(z_-)G(z_-)F_z(z_+)}{U(z_+)G(z_+)F_z(z_-)+U(z_-)G(z_-)F_z(z_+)}, \quad (18)$$

and we can see that neither the multiplicative function G nor the phase-space factor F_z can be eliminated.

In current experiments [29–31], cases i) and ii) are realized, and Eq. (14) can be used to calculate asymmetries. Moreover, at fixed values of x and y, it is valid in a wide range of the ρ values. Condition iii), requiring that Eq. (18) must be used, is satisfied only in small regions near ρ_+ and ρ_-. In our numerical calculations for the system $\hat{K}$, we restrict ourselves to conditions i) and ii).

3. THE BEAM SINGLE-SPIN ASYMMETRY

In calculating the beam single-spin asymmetry, we consider only the case with a longitudinally polarized electron because the respective effect for the transverse polarization of the electron is suppressed by the electron mass.

The cross section of process (1) caused by the BH amplitude can be written in terms of a contraction of the leptonic $L_{\mu\nu}$ and hadronic $H_{\mu\nu}$ tensors,

$$d\sigma = \frac{\alpha^3}{\pi^2 V}L_{\mu\nu}H_{\mu\nu}\,dF. \quad (19)$$

The hadronic tensor is determined by the Dirac (F_1) and Pauli (F_2) proton form factors, which are real in the space-like region, and by the target polarization 4-vector S_μ,

$$H_{\mu\nu} = \frac{1}{4}\mathrm{Tr}(\hat{p}_2+M)\Gamma_\mu(\hat{p}_1+M)(1-\gamma_5\hat{S})\Gamma_\nu,$$
$$\Gamma_\mu = (F_1+F_2)\gamma_\mu-\frac{(p_{1\mu}+p_{2\mu})}{2M}F_2, \quad (20)$$

where M is the proton mass. It is convenient to write it as a sum of the real symmetric polarization-independent and imaginary antisymmetric polarization-dependent parts,

$$H_{\mu\nu} = H_{(\mu\nu)}+iH_{[\mu\nu]},$$

$$H_{(\mu\nu)} = -\frac{V\rho}{2}(F_1+F_2)^2\tilde{g}_{\mu\nu}+$$
$$+2\left(F_1^2+\frac{\rho}{4\tau}F_2^2\right)\tilde{p}_{1\mu}\tilde{p}_{1\nu}, \quad (21)$$

$$H_{[\mu\nu]} = -(\mu\nu q\lambda)M(F_1+F_2)\times$$
$$\times\left[\left(F_1-\frac{\rho}{4\tau}F_2\right)S_\lambda+\frac{(Sp_2)p_{1\lambda}}{2M}F_2\right],\quad q=p_1-p_2, \qquad (22)$$

where we use ( ) and [ ] to denote symmetric and antisymmetric parts of second-rank tensors and

$$\tilde g_{\mu\nu}=g_{\mu\nu}-\frac{q_\mu q_\nu}{q^2},\quad \tilde p_{1\mu}=p_{1\mu}-\frac{(p_1q)q_\mu}{q^2},$$
$$(\mu\nu q\lambda)=\epsilon_{\mu\nu\rho\lambda}q_\rho,\quad \epsilon_{0123}=1.$$

The general structure of the leptonic tensor, accounting for the one-loop radiative correction, can be written as

$$L_{\mu\nu}=B_{(\mu\nu)}+iP_{[\mu\nu]}+$$
$$+\frac{\alpha}{4\pi}\left[B^{(1)}_{(\mu\nu)}+iB^{(1)}_{[\mu\nu]}+iP^{(1)}_{[\mu\nu]}+P^{(1)}_{(\mu\nu)}\right], \qquad (23)$$

where B (P) denotes the unpolarized (spin-dependent) part in the Born approximation and the superscript (1) corresponds to the one-loop correction contribution.

The contraction of tensors in Eq. (19) in the case of the polarized beam and unpolarized proton target is

$$H_{\mu\nu}L_{\mu\nu}=H_{(\mu\nu)}\left[B_{(\mu\nu)}+\frac{\alpha}{4\pi}\left(B^{(1)}_{(\mu\nu)}+P^{(1)}_{(\mu\nu)}\right)\right], \qquad (24)$$

whereas for the polarized target and unpolarized electron beam, we have

$$H_{\mu\nu}L_{\mu\nu}=\left(H_{(\mu\nu)}+iH_{[\mu\nu]}\right)\times$$
$$\times\left[B_{(\mu\nu)}+\frac{\alpha}{4\pi}\left(B^{(1)}_{(\mu\nu)}+B^{(1)}_{[\mu\nu]}\right)\right]. \qquad (25)$$

Therefore, the single-spin beam asymmetry is defined by the formula

$$A_b=\frac{\alpha}{4\pi}\frac{H_{(\mu\nu)}P^{(1)}_{(\mu\nu)}dF}{H_{(\mu\nu)}B_{(\mu\nu)}dF}, \qquad (26)$$

and the single-spin target asymmetry is given by

$$A_t=\frac{\alpha}{4\pi}\frac{H_{[\mu\nu]}B^{(1)}_{[\mu\nu]}dF}{H_{(\mu\nu)}B_{(\mu\nu)}dF}, \qquad (27)$$

where we neglect terms of the order α in the denominator. We recall that for the system K, we can eliminate the phase space dF in the right-hand sides of Eqs. (26) and (27), but this cannot be done in the system $\hat K$ in the general case.

The experimental conditions in reaction (1) are such that the photon has a sufficiently large energy and flies at large angles with respect to both the incoming and outgoing electrons. We can therefore neglect the electron mass (wherever possible) in expressions for both the unpolarized and spin-dependent parts of the lepton tensor.

The unpolarized part in the Born approximation is well-known and is given by

$$B_{(\mu\nu)}=\frac{(s+u)^2+(t+u)^2}{st}\tilde g_{\mu\nu}+$$
$$+\frac{4q^2}{st}\left(\tilde k_{1\mu}\tilde k_{1\nu}+\tilde k_{2\mu}\tilde k_{2\nu}\right), \qquad (28)$$

$$u=-2k_1k_2,\quad s=2kk_2,\quad t=-2kk_1,$$

$$q^2=s+t+u,\quad |u|,|t|,|q^2|,s\gg m^2.$$

The loop correction to the spin-dependent part of the leptonic tensor in the case of a longitudinally polarized electron beam has the structure

$$iP^{(1)}_{[\mu\nu]}+P^{(1)}_{(\mu\nu)}=i\Big[P_{[\mu\nu]}D+(k_1q\nu\mu)(A_1+A_1^*)+$$
$$+(k_2q\nu\mu)(A_2+A_2^*)+$$
$$+(k_1k_2q\nu)\big(B_1\tilde k_{1\mu}+B_2\tilde k_{2\mu}\big)-(k_1k_2q\mu)\big(B_1\tilde k_{1\nu}+B_2\tilde k_{2\nu}\big)\Big],$$

where all the functions D, A_i, and B_i depending on the invariants s, t, and u in limit case $m\to 0$ considered here have been calculated in [24]. We note that the function D is purely real, whereas the functions A_i and B_i have real and imaginary parts. After short simplification, we derive

$$P^{(1)}_{[\mu\nu]}=P_{[\mu\nu]}D+$$
$$+\operatorname{Re}\left\{2A_1+\frac{1}{4q^2}\Big[(st-uq^2)B_1-(s+u)^2B_2\Big]\right\}(k_1q\nu\mu)+$$
$$+\operatorname{Re}\left\{2A_2+\frac{1}{4q^2}\Big[(u+t)^2B_1-(st-uq^2)B_2\Big]\right\}\times$$
$$\times(k_2q\nu\mu), \qquad (29)$$

$$P^{(1)}_{(\mu\nu)}=-\operatorname{Im}\Big\{[(k_1k_2q\mu)\tilde k_{1\nu}+(k_1k_2q\nu)\tilde k_{1\mu}]B_1+$$
$$+[(k_1k_2q\mu)\tilde k_{2\nu}+(k_1k_2q\nu)\tilde k_{2\mu}]B_2\Big\}. \qquad (30)$$

The imaginary parts of B_1 and B_2 appear due to the interference of the Born diagrams in Fig. 1 *a, b* with one loop-corrected diagrams in Fig. 2. In accordance with the results in [24], the quantity B_1 is given by

$$B_1 = \frac{2}{st}\left[\frac{8u}{a}\left(1-\frac{q^2}{a}L_{qu}\right)+ \right.$$
$$+\frac{6t}{b}L_{qt}+\frac{2(u^2-2s^2-su)}{cu}L_{sq}+$$
$$+\frac{2b}{c}\left(1+\frac{s}{c}L_{sq}\right)+\frac{2}{s}(2c-s)L_{tu}+$$
$$+\left(-2-\frac{4c^2}{st}-\frac{12b}{t}-\frac{4s^2}{ut}\right)L_{qu}+\frac{4b^2}{ut}L_{su}+$$
$$\left.+\left(-2+\frac{2uc}{s^2}-\frac{2t}{s}\right)G+\left(\frac{2b}{t}+\frac{2b^2}{t^2}\right)\widetilde{G}+6\right], \quad (31)$$

where we use the same notation as in [24] (see also [25]):

$$(k_1k_2q\sigma)=\epsilon_{\alpha\beta\lambda\sigma}k_{1\alpha}k_{2\beta}q_\lambda, \quad a=s+t,$$
$$b=s+u, \quad c=t+u,$$

$$G = L_{qu}(L_q+L_u-2L_t)-\frac{\pi^2}{3}-$$
$$-2\mathrm{Li}_2\left(1-\frac{q^2}{u}\right)+2\mathrm{Li}_2\left(1-\frac{t}{q^2}\right),$$

$$L_{xy}=L_x-L_y, \quad L_q=\ln\left(-\frac{q^2}{m^2}\right), \quad L_u=\ln\left(-\frac{u}{m^2}\right),$$
$$L_t=\ln\left(-\frac{t}{m^2}\right), \quad L_s=\ln\left(-\frac{s}{m^2}\right).$$

The quantities B_2 and $\widetilde{G}$ can be derived from B_1 and G by the simple substitution

$$B_2=-B_1(s\leftrightarrow t), \quad \widetilde{G}=G(s\leftrightarrow t).$$

The imaginary part of B_1 is hidden in the terms containing L_s and $\widetilde{G}$ and, in turn, the imaginary part of $\widetilde{G}$ arises due to L_s as well to the Spence function $\mathrm{Li}_2(1-q^2/s)$, whose argument is greater than 1. From the casuality principle, it follows that the imaginary part of a diagram containing a loop integration must be reconstructed by adding an extra small negative imaginary piece to the electron mass. This leads to

$$L_s=\ln\frac{s}{m^2}-i\pi,$$
$$\mathrm{Li}_2\left(1-\frac{s}{q^2}\right)=-\int\limits_0^{1-s/q^2}\frac{dx\,\ln x}{1-x}-\ln\frac{u+t}{q^2}L_{sq}, \quad (32)$$

and therefore,

$$\mathrm{Im}\,\widetilde{G}=2\pi\ln\frac{u+t}{u}.$$

By combining the previous results, we obtain

$$\mathrm{Im}\,B_1=-\frac{2\pi}{st}\bar{B}_1, \quad \mathrm{Im}\,B_2=-\frac{2\pi}{st}\bar{B}_2,$$

$$\bar{B}_1=\frac{2(u^2-2s^2-su)}{uc}+\frac{2bs}{c^2}+\frac{4b^2}{ut}-$$
$$-\left(\frac{4b}{t}+\frac{4b^2}{t^2}\right)\ln\frac{u+t}{u}, \quad (33)$$

$$\bar{B}_2=\frac{6s}{c}-\frac{2(2b-t)}{t}+2\left(-2+\frac{2ub}{t^2}-\frac{2s}{t}\right)\ln\frac{u+t}{u}. \quad (34)$$

It can be verified that the singularities of $\bar{B}_1$ and $\bar{B}_2$ as $t\to 0$, which enter separate terms, disappear in the entire expressions. Moreover, they are proportional to t in this limit. This indicates directly that the loop-corrected diagrams with radiation from the initial electron leg do not contribute to the imaginary part of the BH amplitude. We also note that $\bar{B}_1$ and $\bar{B}_2$ tend to zero as $q^2\to 0$.

We can now express all the contractions that are necessary to compute the single-spin beam asymmetry in terms of the invariant variables,

$$H_{(\mu\nu)}B_{(\mu\nu)}=-\frac{V}{(z-\rho)(z-xy)}\times$$
$$\times\left[\chi_1(F_1+F_2)^2+2\chi_2\left(F_1^2+\frac{\rho}{4\tau}F_2^2\right)\right], \quad (35)$$
$$\chi_1=-\rho\big[2z(z-\rho-xy)+(\rho+xy)^2\big],$$

$$\chi_2=(z-\rho-xy)[2z\tau+\rho(1-y)]+$$
$$+\tau(\rho+xy)^2-\rho[1-z+(1-y)^2],$$

where we also use

$$s=V(z-\rho), \quad t=-V(z-xy),$$

and

$$H_{(\mu\nu)}P^{(1)}_{(\mu\nu)}=-\frac{2\pi V\rho}{(z-\rho)(z-xy)}\times$$
$$\times\left(F_1^2+\frac{\rho}{4\tau}F_2^2\right)\left(C+D\ln\frac{z}{xy}\right)\times$$
$$\times\sqrt{Z}\left[\mp\,\mathrm{sign}(\sin\Phi)\right], \quad (36)$$

where the minus sign in front of the signature function pertains to the system K and the plus sign to the system $\hat{K}$, and here we do not distinguish between the notation for the azimuthal angles in these systems. Other quantities in the right-hand side of Eq. (36) are defined as

$$Z=4xy[\rho(1-y)(1-z)+\tau(z-xy)(\rho-z)]-$$
$$-[\rho(1-xy)-y(z-x)]^2,$$

$$C = \frac{1}{z}\left[z - 2 + xy - \rho - y + \right.$$
$$\left. + \frac{\rho + xy}{z} + \frac{2[\rho - xy(1-y+\rho)]}{z - xy}\right],$$
$$D = \frac{2}{z - xy}\left[y(1-x) - \frac{\rho - xy(1-y+\rho)}{z - xy}\right].$$

In writing Eq. (36), we took into account that

$$(k_1 k_2 p_1 p_2) = \frac{V^2}{4}\left[\mp \operatorname{sign}(\sin\Phi)\right]\sqrt{Z}.$$

It is clear that this quantity is proportional to $\sin\Phi$ and can be expressed in the more transparent form

$$(k_1 k_2 p_1 p_2) = -\frac{V^2}{4}\,\frac{2Ky}{\sqrt{y^2 + 4xy\tau}}\sin\Phi \qquad (37)$$

for the system K and

$$(k_1 k_2 p_1 p_2) = \frac{V^2}{4}\times$$
$$\times\, 2\sqrt{[xy(1-y-xy\tau)(\rho - \rho z - z^2\tau)]}\sin\hat{\Phi} \qquad (38)$$

for the system $\hat{K}$. These last equations indicate evidently that the single-spin asymmetry in the BH process tends to zero if all the final particles belong to the same plane provided that the electron beam has the longitudinal polarization. Only the normal beam asymmetry can be nonzero in this case, but it is suppressed by the electron mass.

By combining (26), (35), and (36), we calculate the single-spin asymmetry in the BH process, and our results are shown in Fig. 4.

We see that this asymmetry is of the order 10^{-4} for the considered experimental conditions and reaches a maximum (about four times bigger) at middle values of ρ at fixed values of x and y. The curves for the coordinate systems K and $\hat{K}$ slightly differ in form but are opposite in sign in accordance with Eq. (36). We can assume that the respective effect represents only a small background to the total single-spin beam asymmetry in process (1) caused mainly by the interference between the BH and the imaginary part of VCS amplitudes for a longitudinally polarized electron beam.

4. THE SINGLE-SPIN TARGET ASYMMETRIES

To compute the single-spin target asymmetries in the BH process, we have to find the tensor $B^{(1)}_{[\mu\nu]}$ that is related to the imaginary antisymmetric part of the unpolarized leptonic tensor (see Eq. (27)). The one-loop correction to the spin-independent part of the leptonic tensor has been considered in [25], where it was written as

$$iB^{(1)}_{[\mu\nu]} + B^{(1)}_{(\mu\nu)} = (T_g + T_g^*)\tilde{g}_{\mu\nu} + (T_{11} + T_{11}^*)\tilde{k}_{1\mu}\tilde{k}_{1\nu} +$$
$$+ (T_{22} + T_{22}^*)\tilde{k}_{2\mu}\tilde{k}_{2\nu} +$$
$$+ (T_{12} + T_{21}^*)\tilde{k}_{1\mu}\tilde{k}_{2\nu} + (T_{21} + T_{12}^*)\tilde{k}_{2\mu}\tilde{k}_{1\nu}.$$

The functions T_g and T_{ik} are derived in [25].

It is easy to divide the right-hand side of the above equation into its symmetric and antisymmetric pieces, and we obtain

$$B^{(1)}_{(\mu\nu)} = \operatorname{Re}\left[2(T_g\tilde{g}_{\mu\nu} + T_{11}\tilde{k}_{1\mu}\tilde{k}_{1\nu} + T_{22}\tilde{k}_{2\mu}\tilde{k}_{2\nu}) + \right.$$
$$\left. + (T_{12} + T_{21})(\tilde{k}_1\tilde{k}_2)_{\mu\nu}\right],$$

$$B^{(1)}_{[\mu\nu]} = \operatorname{Im}(T_{12} - T_{21})[\tilde{k}_1\tilde{k}_2]_{\mu\nu}. \qquad (39)$$

Neglecting terms that contain the squared electron mass, we have

$$T_{12} = \frac{2}{st}\left[\frac{cq^2(u-s)G}{s^2} + \frac{q^2(uq^2 - st)\widetilde{G}}{t^2} - \right.$$
$$- 2q^2\left(\frac{uq^2}{st} + \frac{2u - s + t}{a}L_{qu}\right) + 8u + 3t - s +$$
$$+ \frac{2us}{c} - \frac{4(u^2 - cs)(q^2 L_{qu} - a)}{a} +$$
$$\left. + \frac{q^2(2c + t)(st - uq^2)}{c^2 t}L_{qs} - \frac{q^2 c(2u - s)}{bs}L_{qt}\right], \qquad (40)$$

and T_{21} can be obtained from T_{12} by the substitution $T_{21} = T_{12}(s \leftrightarrow t)$. By means of rule (32), we can extract the imaginary part and write

$$B^{(1)}_{[\mu\nu]} = 2\pi(\tilde{k}_{1\mu}\tilde{k}_{2\nu} - \tilde{k}_{1\nu}\tilde{k}_{2\mu})T,$$
$$T = \frac{q^2}{st}\left[\frac{2st}{c^2} + 4u\left(\frac{1}{t}\ln\frac{u+t}{u} - \frac{1}{c}\right)\right]. \qquad (41)$$

In the same manner as $\bar{B}_1$ and $\bar{B}_2$ in Sec. 3, the quantity T does not have a singularity as $t \to 0$ and tends to zero as $q^2 \to 0$.

The contraction of the hadronic and leptonic tensors in the numerator of the right-hand side of Eq. (27) is given by

$$H_{[\mu\nu]}B^{(1)}_{[\mu\nu]} = -\frac{4\pi M\rho(F_1 + F_2)}{V(z-\rho)(z-xy)}\times$$
$$\times\left(-1 + \frac{\rho - xy}{z} + \frac{xy\rho}{z^2} + \frac{2xy}{z - xy}\ln\frac{z}{xy}\right)G_s, \qquad (42)$$

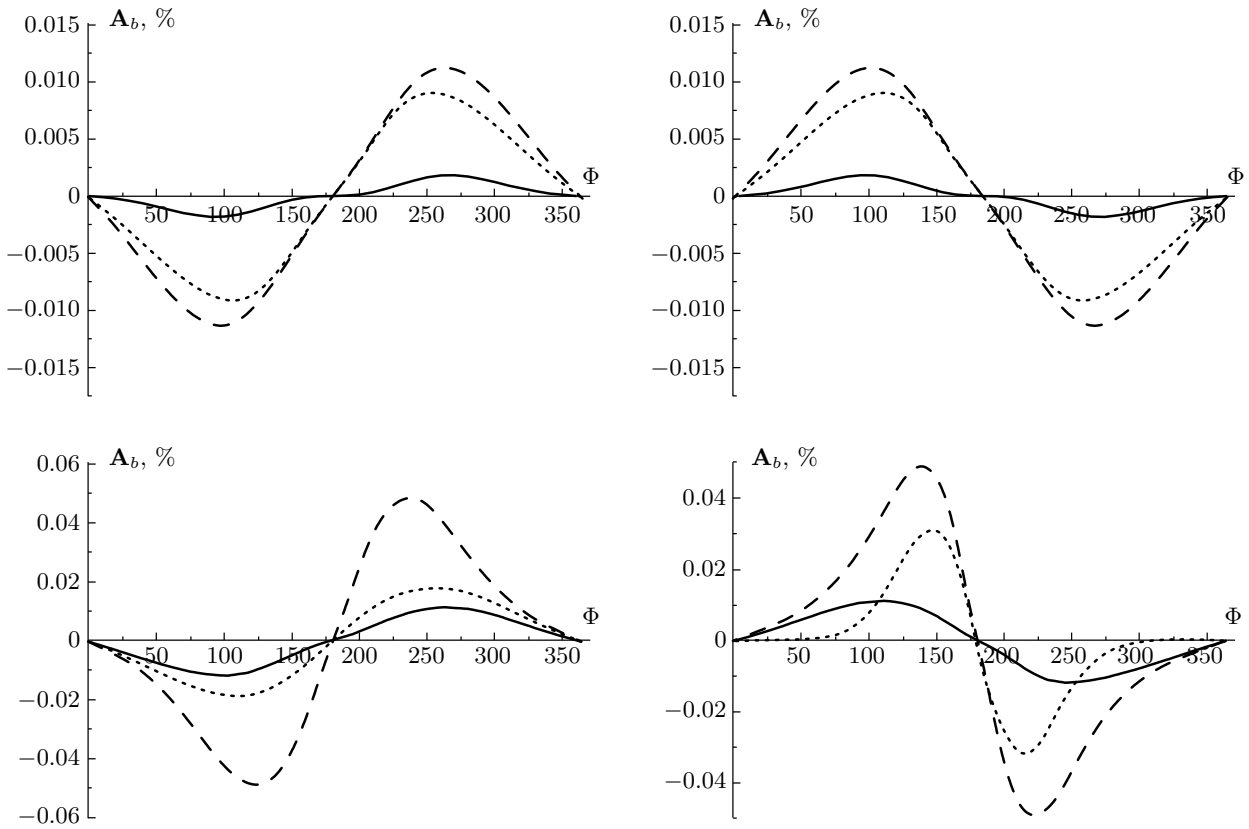

Fig. 4. Dependence of the single-spin beam asymmetry on the azimuthal angle (in degrees) for three different experimental conditions (top panel): $x = 0.19$, $y = 0.825$, $\rho = 0.024$ for CLAS1 [29] (solid lines), $x = 0.18$, $y = 0.5$, $\rho = 0.0185$ for CLAS2 [30] (dashed lines), and $x = 0.11$, $y = 0.458$, $\rho = 0.005$ for HERMES [31] (dotted lines). Curves for different values of $\rho = 0.0185$ (solid lines), 0.2 (dashed lines), 0.42 (dotted lines) on the bottom panel are suitable under CLAS2 conditions. The left column corresponds to the system K, and the right one to the system $\hat{K}$

where the quantity G_s depends on the target-proton polarization 4-vector S,

$$G_s = 2(k_1k_2qS)\left(F_1 - \frac{\rho}{4\tau}F_2\right) + \frac{(k_1k_2qp_1)(p_2S)}{V\tau}F_2.$$

To calculate the target single-spin asymmetries, we must know the polarization vector S_μ. In general, the one-loop correction to the leptonic part of the interaction generates different types of such an asymmetry.

If the longitudinal (L) target proton polarization in laboratory system is chosen along the direction of $\mathbf{k}_1$, the transverse (T) polarization in the plane $(\mathbf{k}_1, \mathbf{k}_2)$, and the normal ($N$) one along the direction of $\mathbf{k}_1 \times \mathbf{k}_2$, then the respective polarization 4-vectors $S_1^{(L,T,N)}$ can be expressed through the particle 4-momenta as [32]

$$\begin{aligned} S^L_{1\mu} &= \frac{2\tau k_{1\mu} - p_{1\mu}}{\sqrt{V\tau}}, \\ S^N_{1\mu} &= -\frac{2(\mu k_1 k_2 p_1)}{\sqrt{V^3 xy(1-y-xy\tau)}}, \\ S^T_{1\mu} &= \frac{k_{2\mu} - (1-y-2xy\tau)k_{1\mu} - xyp_{1\mu}}{\sqrt{Vxy(1-y-xy\tau)}}, \end{aligned} \tag{43}$$

where

$$(S_1^I S_1^J) = -\delta_{IJ}, \quad (S_1^I p_1) = 0, \quad I, J = L, T, N.$$

For this choice of the target polarization, we have

$$G^L_{s1} = -\frac{(k_1k_2qp_1)}{\sqrt{V\tau}}\Big(2F_1 + zF_2\Big), \tag{44}$$

$$G^T_{s1} = \frac{(k_1k_2qp_1)}{\sqrt{Vxy(1-y-xy\tau)}} \times \times \left[-2xyF_1 + \frac{F_2}{2\tau}\big(\rho + xy - yz(1+2x\tau)\big)\right], \tag{45}$$

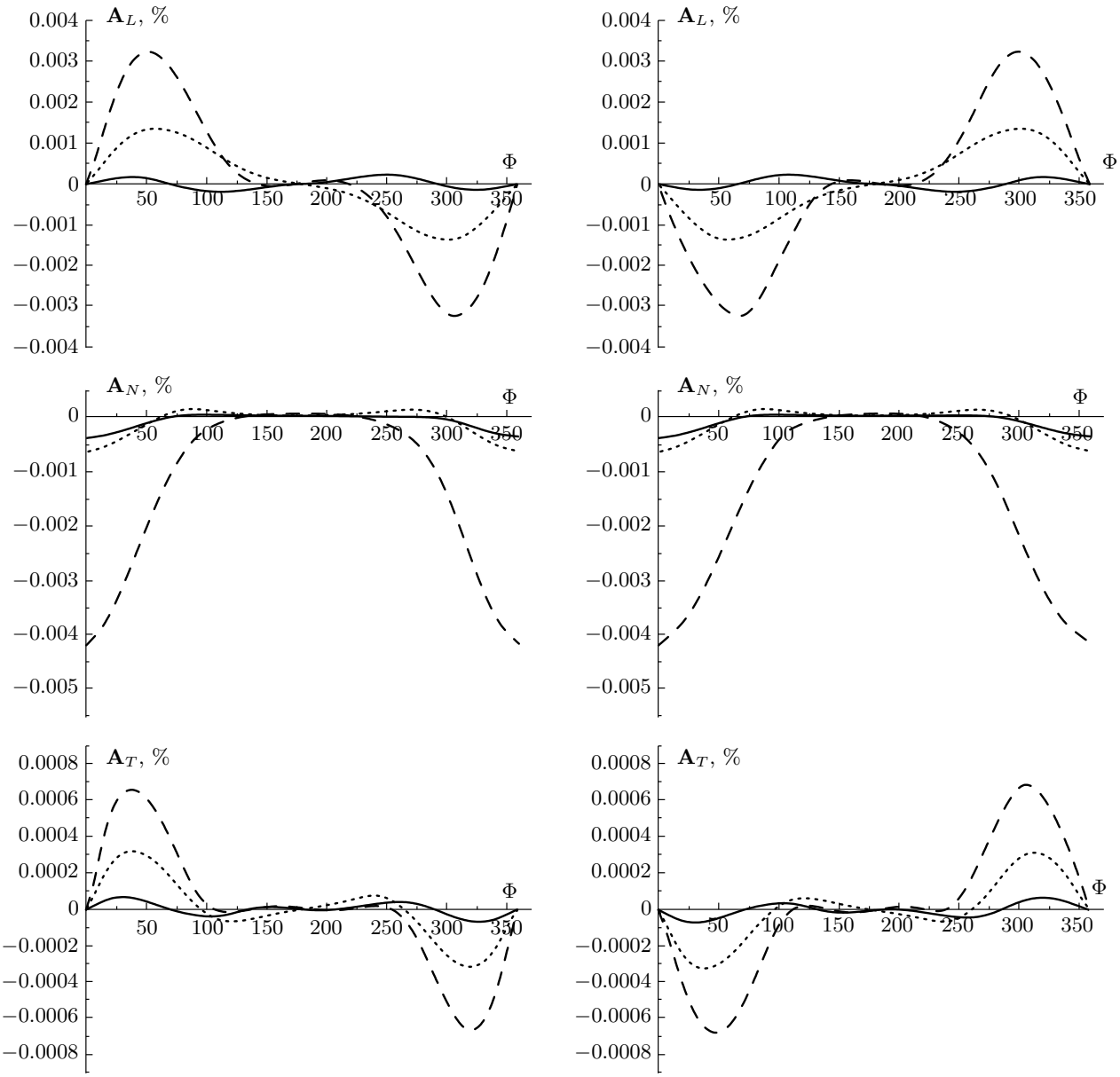

Fig. 5. The target single-spin asymmetries that are suitable for choice (43) of the target-proton polarizations for different experimental conditions: CLAS1 (solid lines), CLAS2 (dashed lines), and HERMES (dotted lines). The left column corresponds to the system K, and the right one to the system $\hat{K}$

$$G_{s1}^N = -\frac{1}{2}\sqrt{\frac{V^3 xy}{(1-y-xy\tau)}}\left\{\left(F_1 - \frac{\rho}{4\tau}F_2\right)\times\right.$$
$$\left.\times\,[z(2-y)-\rho-xy(1-\rho)]-\frac{4F_2(k_1k_2qp_1)^2}{V^4 xy\tau}\right\}, \quad (46)$$

where the proton form factors depend on

$$q^2 = -Q^2 = -\rho V.$$

For the quanity $(k_1k_2qp_1)$, we have to use Eq. (37) if the system K is taken or Eq. (38) in the case of the system $\hat{K}$. The target single-spin asymmetries corresponding to polarizations (43) are shown in Figs. 5, 6. The left column corresponds to the K system and the right one to $\hat{K}$.

The absolute values of the target asymmetries A_L and A_T are about one order smaller than the beam asymmetry but strongly depend on the value of ρ. The normal target asymmetry is nonzero when $\sin\Phi = 0$, which is not surprising because such a parity-conser-

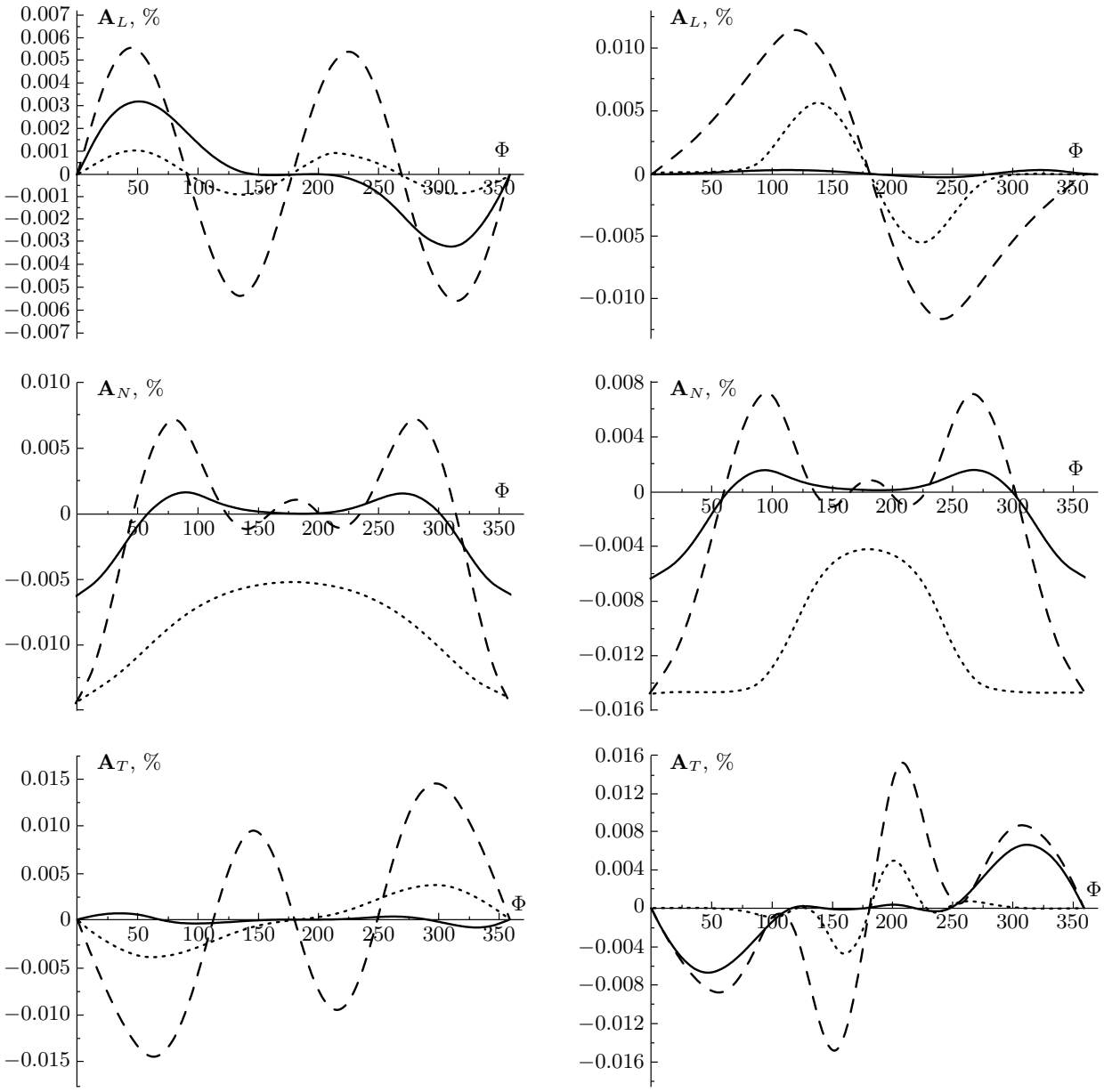

Fig. 6. The ρ-dependence of the target asymmetry for the polarization choice in (43). The left column (system K) from top down: CLAS2, HERMES, CLAS1; the right column (system $\hat{K}$): CLAS1, HERMES, CLAS2

ved asymmetry exists even in elastic electron–proton scattering where the outgoing electron and the recoil proton belong to the same plane.

Another often used choice of directions to define target polarizations in laboratory system is as follows. The longitudinal direction can be taken along the 3-momentum $\mathbf{p}_2$, the transverse one in the plane $(\mathbf{k}_1, \mathbf{p}_2)$, and the normal direction along the 3-vector $\mathbf{p}_2 \times \mathbf{k}_1$. The covariant expressions for the respective polarization 4-vectors are [33]

$$S^L_{2\mu} = \frac{-2\tau q_\mu - \rho p_{1\mu}}{\sqrt{V\tau\rho(4\tau+\rho)}}, \quad S^N_{2\mu} = -\frac{2(\mu p_2 k_1 p_1)}{\sqrt{V^3\eta}}, \quad \eta = \rho(1-z) - z^2\tau, \tag{47}$$

$$S^T_{2\mu} = \frac{\rho(4\tau+\rho)k_{1\mu} + (\rho+2z\tau)q_\mu - \rho(2-z)p_{1\mu}}{\sqrt{V\eta\rho(4\tau+\rho)}}.$$

These 4-vectors are orthogonal and satisfy the same normalization and transversality conditions as the 4-vectors $S^I_{1\mu}$. With this choice, we have

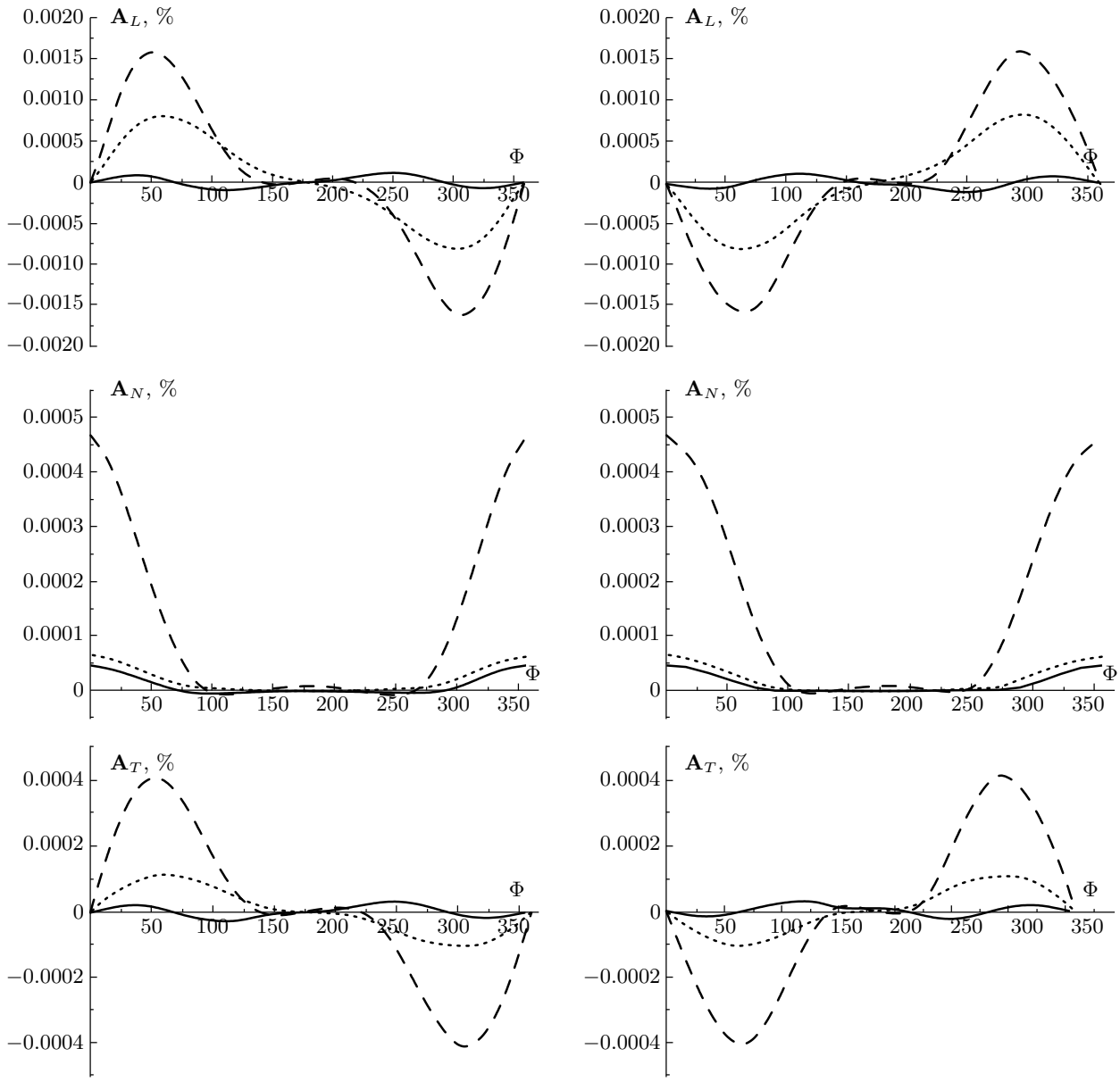

Fig. 7. The same as in Fig. 5 but for the parameterization of the target proton polarization given by (47)

$$G_{s2}^{L} = -2\sqrt{\frac{\rho}{V\tau(4\tau+\rho)}}(k_1k_2qp_1)(F_1+F_2), \qquad (48)$$

$$G_{s2}^{T} = -2\sqrt{\frac{\rho}{V\eta(4\tau+\rho)}}(k_1k_2qp_1)(2-z)\times \times\left(F_1-\frac{\rho}{4\tau}F_2\right), \qquad (49)$$

$$G_{2s}^{N} = \frac{1}{2}\sqrt{\frac{V^3}{\eta}}\{\rho[2xy-z(1+xy)]-yz(x-z)\}\times \times\left(F_1-\frac{\rho}{4\tau}F_2\right). \qquad (50)$$

The target asymmetries corresponding to parameterization (47) of the proton polarization are represented in Figs. 7, 8. The longitudinal and transverse asymmetries are about two times smaller than in the previous case, whereas the normal one is smaller by an order of magnitude.

We note that combinations of form factors that enter G_{s2}^{L} and $G_{s2}^{T,N}$ are exactly the Sachs electric and magnetic ones [34],

$$F_1+F_2=G_M, \quad F_1-\frac{\rho}{4}\tau F_2=G_E.$$

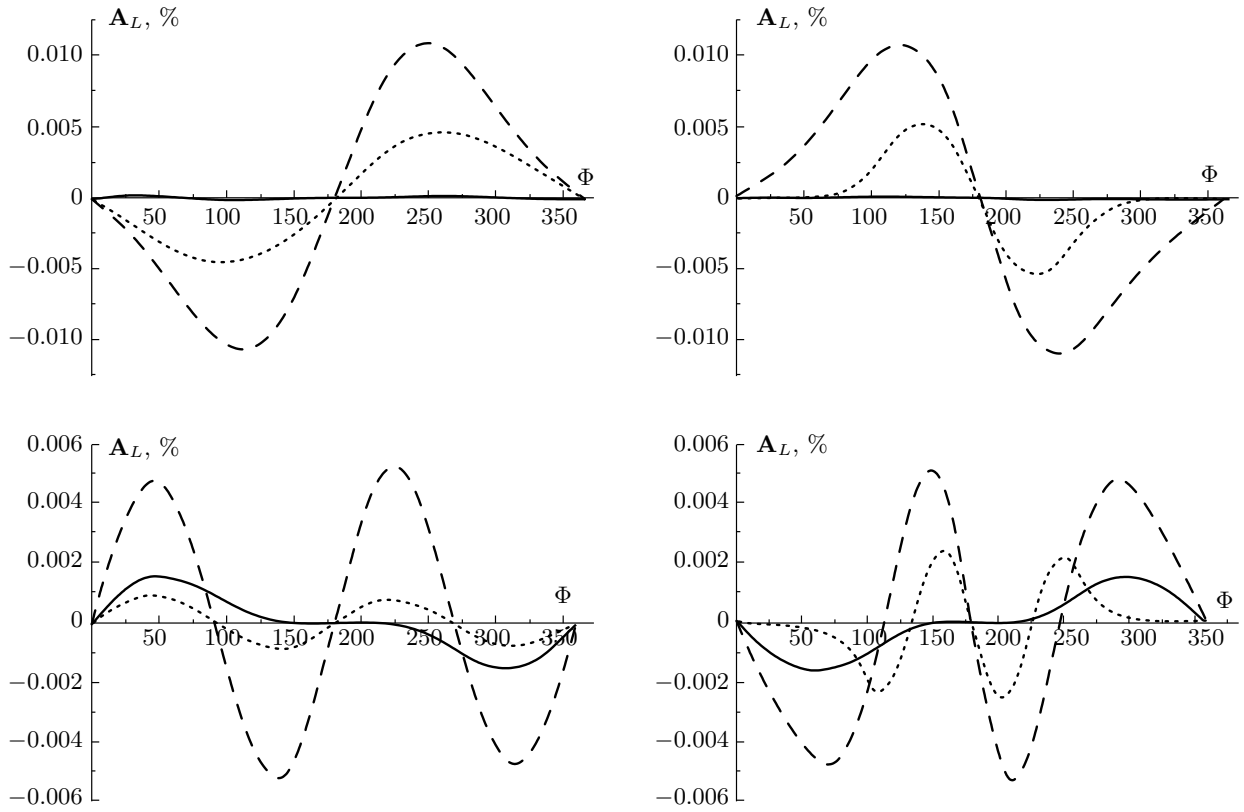

Fig. 8. The longitudinal target asymmetry for the CLAS2 conditions at different values of ρ at fixed x and y for the polarization choice in (47). The left column corresponds to the system K and the right one to the system $\hat{K}$

That is why the target single-spin asymmetries in the BH process for the polarization chosen as in Eq. (47) can be used, in principle, for independent determination of the proton form factors. The corresponding experiments with transferred polarization from the electron to the recoil proton in elastic *ep*-scattering [35] require an analysis of the secondary scattering [36] that involves the loss of a few orders of magnitude in the count rate. The number of events that contribute to the single-spin correlation in the BH process is of the order α^2 compared with the elastic scattering, but the secondary scattering is not necessary.

Our calculations indicate that single-spin beam and target asymmetries generated by loop corrections to the leptonic part of the interaction in the BH process are very small and do not exceed $6 \cdot 10^{-4}$ for the experimental conditions considered here. The reason is that in addition to the fine structure constant, they contain kinematical suppression due to the chosen values of invariant variables. Thus, we conclude that the considered effect gives a small contribution to the total radiative correction in process (1), which mainly probes the virtual Compton scattering amplitude and can reach about 5 % [23].

REFERENCES

1. P. A. M. Guichon, G. Q. Liu, and A. W Thomas, Nucl. Phys. A **591**, 606 (1995).
2. D. Drechel, G. Knöchlein, A. Yu. Korchin, A. Metz, and S. Scherer, Phys. Rev. C **57**, 941 (1998); Phys. Rev. C **58**, 1751 (1998); A. Yu. Korchin and O. Scholten, Phys. Rev. C **58**, 1098 (1998).
3. G. Q. Liu, A. W. Thomas, and P. A. M. Guichon, Austral. J. Phys. **49**, 905 (1996).
4. M. Vanderhaeghen, Phys. Lett. B **368**, 13 (1996).
5. M. Metz and D. Drechel, Z. Phys. A **356**, 351 (1996); Z. Phys. A **359**, 165 (1997).
6. T. R. Hemmert, B. R. Holstein, G. Knöchlein, and S. Scherer, Phys. Rev. D **55**, 2630 (1997); Phys. Rev. Lett. **79**, 22 (1997).

7. B. Pasquini and G. Salme, Phys. Rev. C **57**, 2589 (1998).

8. J. Roche, J. M. Friedrich, D. Lhuillier et al., Phys. Rev. Lett. **85**, 708 (2000); J. M. Friedrich, P. Bartsch, D. Baumann et al., Nucl. Phys. A **663**, 389 (2000).

9. R. Van de Vyver, Nucl. Phys. A **669**, 192 (2002).

10. D. Müller et al., Fortschr. Phys. **42**, 2 (1994).

11. A. V. Radyushkin, Phys. Lett. B **385**, 333 (1996); Phys. Rev. D **56**, 5524 (1997).

12. X. Ji, Phys. Rev. Lett. **78**, 610 (1997); J. Phys. G **24**, 1181 (1998).

13. M. Diehl, Phys. Rep. **388**, 41 (2003); A. V. Belitsky and A. V. Radyushkin, E-print archives hep-ph 0504030.

14. P. Y. Bertin, G. Hyde-Wright, and Y. Roblin, *Proc. of the Conf. «Nuclear and Particle Physics with CEBAF at JLAB»*, Dubrovnik (1998); Fyzika B **8**, 207 (1999).

15. N. d'Hose, E. Burtin, P. A. M. Guichon, and J. Marroncle, Eur. Phys. J. A **19**, 47 (2004).

16. L. W. Mo and Y. S. Tsai, Rev. Mod. Phys. **41**, 205 (1969); L. C. Maximon and J. A. Tjon, Phys. Rev. C **62**, 054320 (2000).

17. Y. C. Chen, A. V. Afanasev, S. J. Brodsky, C. E. Carlson, and M. Vanderhaeghen, Phys. Rev. Lett. **93**, 122301 (2004).

18. N. F. Mott, Proc. R. Soc. London A **135**, 429 (1935); A. O. Barut and C. Fronsdal, Phys. Rev. **120**, 1871 (1960); A. De Rujula, J. M. Kaplan, and E. De Rafael, Nucl. Phys. B **35**, 365 (1971).

19. T. V. Kukhto, S. N. Panov, E. A. Kuraev, and A. A. Sazonov, Preprint JINR-E2-92-556 (1993).

20. M. Gorstein, P. A. M. Guichon, and M. Vanderhaeghen, Nucl. Phys. A **741**, 234 (2004).

21. A. V. Afanasev and N. P. Merenkov, Phys. Rev. D **70**, 073002 (2004); Phys. Lett. B **599**, 48 (2004).

22. SAMPLE Collaboration, S. P. Wells et al., Phys. Rev. C **63**, 064001 (2001); MAMI/A4 Collaboration, F. Maas et al. (unpublished); SLAC E 158 Experiment, contact person K. Kumar; G. Gates, K. Kumar, and D. Lhuiller, spokespersons, HAPPEX-2 Experiment, Jlab Report № E-99-115; D. Beck spokesperson, JLab/G0 Experiment, JLab Reports № E-00-006 and № E-01-016.

23. M. Vanderhaeghen, J. M. Friedrich, D. Lhuillier et al., Phys. Rev. C **62**, 025501 (2000).

24. I. Akushevich, A. Arbuzov, and E. Kuraev, Phys. Lett. B **432**, 222 (1998).

25. E. A. Kuraev, N. P. Merenkov, and V. S. Fadin, Yad. Fiz. **45**, 782 (1987).

26. J. H. Kühn and G. Rodrigo, Eur. Phys. J. C **25**, 215 (2002).

27. A. V. Belitsky, D. Müller, and A. Kirchner, Nucl. Phys. B **629**, 323 (2002).

28. M. Diehl and S. Sapeta, E-print archives hep-ph/0503023.

29. S. Stepanyan [CLAS Collaboration], Phys. Rev. Lett. **87**, 182002 (2001).

30. E. S. Smith [CLAS Collaboration], AIP Conf. Proc. **698**, 129 (2004) E-print archives nucl-ex/0308032.

31. A. Airapetyan, N. Akopov, Z. Akopov et al., Phys. Rev. Lett. **87**, 182001 (2001).

32. A. V. Afanasev, I. Akushevich, and N. P. Merenkov, Zh. Eksp. Teor. Fiz. **98**, 403 (2004).

33. A. V. Afanasev, I. Akushevich, and N. P. Merenkov, Phys. Rev. D **65**, 013006 (2002).

34. R. G. Sachs, Phys. Rev. **74**, 433 (1448).

35. M. K. Jones, K. A. Aniol, F. T. Baker et al., Phys. Rev. Lett. **84**, 1398 (2000); O. Gayou, E. J. Brash, M. K. Jones et al., Phys. Rev. Lett. **88**, 092301 (2002).

36. R. G. Arnold, C. E. Carlson, and F. Gross, Phys. Rev. C **23**, 363 (1981).